Effect of volume ratio on thermocapillary flow in liquid bridges of high-Prandtl-number fluids

Bo Xun, Kai Li,* and Wen-Rui Hu

Key Laboratory of Microgravity, Institute of Mechanics, Chinese Academy of Sciences, Beijing 100190, China and National Microgravity Laboratory, Institute of Mechanics, Chinese Academy of Sciences, Beijing 100190, China

(Received 13 September 2009; revised manuscript received 18 December 2009; published 26 March 2010)

In present study, the transition of thermocapillary convection from the axisymmetric stationary flow to oscillatory flow in liquid bridges of 5cst silicon oil (aspect ratio 1.0 and 1.6) is investigated in microgravity conditions by the linear instability analysis. The corresponding marginal instability boundary is closely related to the gas/liquid configuration of the liquid bridge noted as volume ratio. With the increasing volume ratio, the marginal instability boundary consists of the increasing branch and the decreasing branch. A gap region exists between the branches where the critical Marangoni number of the corresponding axisymmetric stationary flow increases drastically. Particularly, a unique axisymmetric oscillatory flow (the critical azimuthal wave number is $m=0$) in the gap region is reported for the liquid bridge of aspect ratio 1.6. Moreover, the energy transfer between the basic state and the disturbance fields of the thermocapillary convection is analyzed at the corresponding critical Marangoni number, which reveals different major sources of the energy transfer for the development of the disturbances in regimes of the increasing branch, the gap region and the decreasing branch, respectively.

DOI: 10.1103/PhysRevE.81.036324 PACS number(s): 47.55.nb, 47.20.−k, 81.10.Mx

I. INTRODUCTION

A liquid bridge consisting of a liquid column supported between two differently heated solid rods (see Fig. 1) was initially introduced to mimic half of the floating zone technique for the interests of space materials science. It now has become one of the typical models for the investigation of the principles of thermocapillary convection experimentally and theoretically. With an applied temperature difference (ΔT), the temperature gradient of the gas/liquid interface tension drives the thermocapillary convection in the liquid bridge. With the increasing ΔT, the thermocapillary convection transfers form an axisymmetric stationary flow to an asymmetric stationary flow in liquid bridges of low-Prandtl-number fluids or to an oscillatory flow in liquid bridges of high-Prandtl-number fluids. The corresponding marginal instability boundary depends on a set of parameters. One of the most sensitive parameters is the volume ratio of the liquid bridge [1–5]. In microgravity conditions, a cylindrical liquid bridge is only a special case. The gas/liquid interface (usually noted as free surface) shape could be convex or concave. The curvature variation in the longitudinal direction of the free surface alters the equilibrium of the forces and then the onset of oscillatory thermocapillary convection. The volume ratio is defined as the ratio of the volume of liquid column to that of a cylindrical case of the same height and diameter:

$$V = \frac{1}{R^2}\int_0^L r^2(z)dz,$$

where $h(z)$ is the free-surface boundary in the region of $0 \le z \le L$ and R the radius of the corresponding cylindrical one (see Fig. 1). For liquid bridges of low-Pr fluids, the marginal instability boundary exhibits a convex trend; i.e., the critical Marangoni number first decreases and then increases with the increasing volume ratio [2,3]. For liquid bridges of high-Pr fluids, the marginal instability boundary consists of two branches as typically shown in Fig. 2, the increasing branch in the range of volume ratios approximately less than unity (referred as slender bridge) and the decreasing branch in the range of volume ratios approximately larger than unity (referred as fat bridge) [1,3,5]. Moreover, a strongly stabilized region for the axisymmetric stationary thermocapillary flow exists between the branches. The different trends of the marginal instability boundaries imply the different mechanisms of the instability of the thermocapillary convection in liquid bridges of low-Pr fluids and high-Pr fluids. Although the studies mentioned above have been conducted on the effect of volume ratio on the thermocapillary convection, details of the thermocapillary convection in the strongly stabilized gap region of the marginal instability boundary for liquid bridges of high-Pr fluids are still lacking.

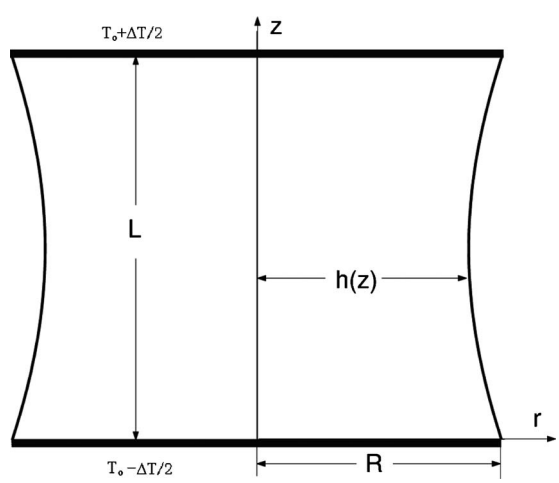

FIG. 1. Scheme diagram of a liquid bridge in microgravity conditions.

*likai@imech.ac.cn

 ©2010 The American Physical Society

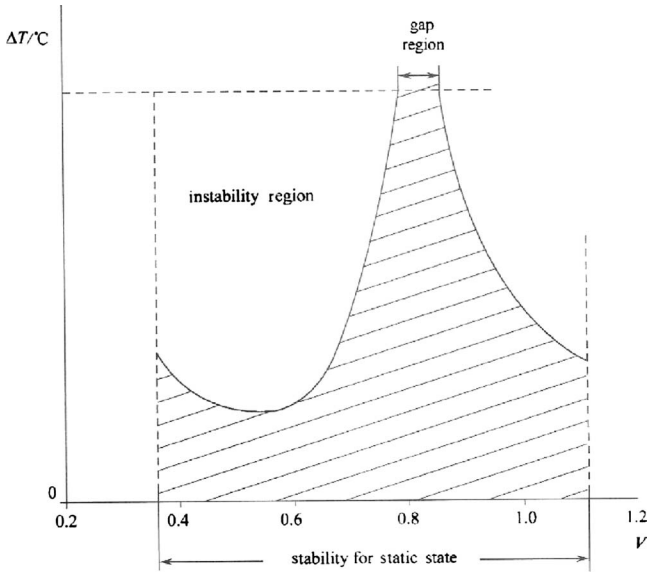

FIG. 2. Scheme diagram of the volume-ratio dependent marginal instability boundary of liquid bridge after [1].

In present study, for liquid bridges of 5cst silicon oil in microgravity conditions, the volume-ratio dependent marginal instability boundary of the thermocapillary convection is investigated by the linear instability analysis, especially the details in the range of the strongly stabilized gap region. Moreover, the energy balance between the basic state and the disturbance of the thermocapillary convection at the critical condition is analyzed. Section II describes the problem and the numerical schemes. The numerical results are given in Sec. III. Conclusions are given in Sec. IV.

II. GOVERNING EQUATIONS AND NUMERICAL SCHEMES

A liquid bridge of 5cst silicon oil (Pr=68.6) with the adiabatic free surface in microgravity conditions is shown in Fig. 1 (The corresponding thermophysical properties are listed in Table I). The liquid bridge is of height L and radius R. The local radius of the free surface is denoted as h(z). The length, velocity, pressure and time are scaled by R, $\gamma\Delta T/\rho\upsilon$, $\gamma\Delta T/R$, and R^2/υ, respectively, and the temperature measured with respect to T_0 is scaled by ΔT where ρ is the density of the fluid, υ the kinematic viscosity coefficient, γ the negative temperature gradient of surface tension, and T_0 the mean temperature of the upper and lower rods.

In the cylindrical coordinates (r, θ, z), the nondimensional governing equations are as follows:

$$\vec{\nabla} \bullet \vec{U} = 0 \tag{1}$$

TABLE I. Thermophysical properties of 5cst silicone oil.

ρ	915 $(\mathrm{kg/m^3})$	υ	5×10^{-6} $(\mathrm{m^2/s})$
γ	5.6×10^{-5} $(\mathrm{kg/K\times s^2})$	α	7.29×10^{-8} $(\mathrm{m^2/s})$

$$\frac{\partial \vec{U}}{\partial t} + \frac{\mathrm{Ma}}{\mathrm{Pr}}(\vec{U} \bullet \vec{\nabla})\vec{U} + \vec{\nabla}P = \Delta\vec{U} \tag{2}$$

$$\frac{\partial T}{\partial t} + \frac{\mathrm{Ma}}{\mathrm{Pr}}(\vec{U} \bullet \vec{\nabla})T = \frac{1}{\mathrm{Pr}}\Delta T \tag{3}$$

where $\vec{U}=(u, v, w)$ indicates the dimensionless velocity vector, P the pressure, T the temperature, and t the time. The Marangoni number and Prandtl number are defined as $\mathrm{Ma}=\gamma\Delta TR/\rho\upsilon^2$ and $\mathrm{Pr}=\upsilon/\alpha$, respectively, where α the thermal diffusivity coefficient.

The corresponding boundary conditions are as follows:

$$z=0, \quad \Gamma:\vec{U}=0, \quad T=\mp\frac{1}{2}, \tag{4}$$

$$r=\mathrm{h(z)}:\vec{n}\bullet\vec{U}=0, \quad \vec{t}_z\bullet(S\bullet\vec{n}) = -\vec{t}_z\bullet\vec{\nabla}T,$$

$$\vec{t}_\theta\bullet(S\bullet\vec{n}) = -\vec{t}_\theta\bullet\vec{\nabla}T, \quad \vec{n}\bullet\vec{\nabla}T=0. \tag{5}$$

where $\Gamma=L/R$ is the aspect ratio, $S=\vec{\nabla}\vec{U}+(\vec{\nabla}\vec{U})^T$ the stress tensor in nondimensional form, the vector $\vec{n}$ the outward-directed normal vector of the free surface and the vectors $\vec{t}_z$ and $\vec{t}_\theta$ the unit vectors tangent to the free surface in the (r, z) plane and (r, θ) plane, respectively. Regularization of the boundary conditions as in [3] is not introduced in the present study. In the present study, the dynamic free-surface deformation induced by the thermocapillary convection is negligible, therefore, the free-surface shape is independent of the flow and temperature fields and identical to the static axisymmetric shape under the static situation. Then the free-surface shape $h(z)$ can be obtained from the Young-Laplace equation,

$$P_s = \vec{\nabla}\bullet\vec{n}. \tag{6}$$

This second-order ordinary equation for $h(z)$ and the dimensionless pressure jump P_s is solved with the boundary conditions,

$$h(0)=h(\Gamma)=1, \tag{7}$$

and the prescribed volume ratio or, equivalently, the prescribed contact angle at the hot rod,

$$\alpha_h = \frac{\pi}{2} - tg^{-1}\left(\frac{dh(z)}{dz}\right). \tag{8}$$

The problem is solved using the method of linear stability analysis. The axisymmetric stationary flow (basic state) is directly calculated from the steady N-S equations, and then small three-dimensional disturbances are added to the basic state and linearized by neglecting high orders of the disturbances [6–9]. The disturbances are assumed to be in the normal mode,

TABLE II. Grid dependence code validation for liquid bridge of Pr=68.6.

$\Gamma=1.0,\ V=0.74$			$\Gamma=1.6,\ V=0.83$		
$N_r\times N_z$	10^5 Ma$_c$	m	$N_r\times N_z$	10^4 Ma$_c$	m
71×101	2.19	1	61×121	4.99	0
81×115	2.30	1	71×131	5.11	0
91×125	2.40	1	81×141	5.21	0
101×135	2.48	1	91×151	5.30	0

$$\begin{pmatrix}\vec{u}'\\ p'\\ T'\end{pmatrix}=\sum_{m=-\infty}^{+\infty}\begin{pmatrix}\vec{u}'^m(r,z)\\ p'^m(r,z)\\ T'^m(r,z)\end{pmatrix}\exp[\sigma(m)t+jm\theta], \tag{9}$$

where the variables with prime denote the disturbances, m the azimuthal wave number, $\sigma(m)$ the complex growth rate of the corresponding perturbation mode and $j=\sqrt{-1}$. The critical Marangoni number Ma$_c$ is obtained when the maximal real part of $\sigma(m)$ for all m is zero. The problem is numerically solved in the body-fitted curvilinear coordinates with coordinate transformation,

$$\xi=\frac{r}{h(z)}\ .\qquad \eta=z \tag{10}$$

Detailed description of the transformed governing equations can be found in [4]. A more detailed description of the numerical schemes can be found in [10,11]. A code validation of noncylindrical liquid bridges can be found in [7]. The grid numbers used in the calculation are $N_r\times N_z=91\times 125$ for $\Gamma=1.0$ and $N_r\times N_z=81\times 141$ for $\Gamma=1.6$, respectively, where N_r and N_z indicate the numbers of the grid points in radial and axial directions. Increasing density of the grid points is adopted close to both solid boundary and free surface to well resolve the corresponding boundary layers [7]. The grid dependent critical Marangoni numbers for two selected cases is shown in Table II which verifies the present meshes of grid points.

To throw some lights on the physics of the instabilities, changing rates of kinetic (E_k) and "thermal" energy (E_{th}) of the critical disturbances are also investigated [2,6,7]. The disturbance equations of momentum and temperature are multiplied by the velocity and temperature disturbances, respectively, and then integrated over the volume of the liquid bridge (Ω) and normalized by the mechanical (D_k) and thermal dissipation (D_{th}), respectively,

$$\frac{1}{D_k}\frac{dE_k}{dt}=M+I-1=M_r+M_\theta+M_z+I-1, \tag{11}$$

$$\frac{1}{D_{th}}\frac{dE_{th}}{dt}=J-1=J_r+J_z-1. \tag{12}$$

where $E_k=\int_\Omega(\vec{u}'^2/2)d\Omega$, $E_{th}=\int_\Omega(T'^2/2)d\Omega$, $D_k=\int_\Omega(S':S'/2)d\Omega$, and $D_{th}=\int_\Omega(\vec{\nabla}T'\bullet\vec{\nabla}T'/\mathrm{Pr})d\Omega$. $I=-(\mathrm{Ma}/2\ \mathrm{Pr})\int_\Omega\vec{u}'\bullet S\bullet\vec{u}'d\Omega$ is the interaction between the stress tensor of the basic state and the velocity disturbance. $M=-(1/D_k)\int_s\vec{u}'\bullet\vec{\nabla}T'ds$ is the integration over the surface of Ω, which denotes the work related to the thermocapillary force induced by the temperature disturbance on the free surface and can be decomposed in the radial, azimuthal and axial directions, respectively,

$$M_r=-(1/D_k)\int_s u'(\partial T'/\partial r)ds,$$

$$M_\theta=-(1/D_k)\int_s v'(\partial T'/\partial\theta)ds,$$

and

$$M_z=-(1/D_k)\int_s w'(\partial T'/\partial z)ds.$$

$J=-(1/D_{th})(\mathrm{Ma}/\mathrm{Pr})\int_\Omega(\vec{u}'\bullet\vec{\nabla}T)T'd\Omega$ is the energy transfer from the basic temperature field to the temperature disturbance field by the velocity disturbance field and can be decomposed in the radial and axial directions, respectively,

$$J_r=-(1/D_{th})(\mathrm{Ma}/\mathrm{Pr})\int_\Omega(u'(\partial T/\partial r))T'd\Omega,$$

$$J_z=-(1/D_{th})(\mathrm{Ma}/\mathrm{Pr})\int_\Omega(w'(\partial T/\partial z))T'd\Omega.$$

Moreover, the density distribution of J_r and J_z can be introduced as j_r and j_z with $J_r=\int_0^\Gamma dz\int_0^1 j_r dr$ and $J_z=\int_0^\Gamma dz\int_0^1 j_z dr$, respectively.

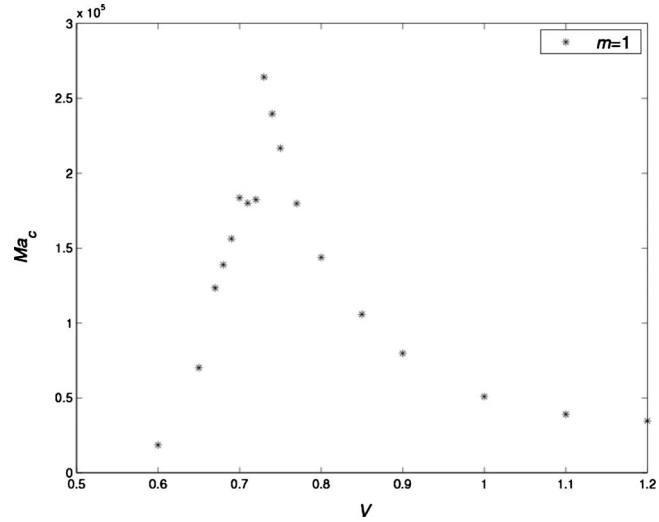

FIG. 3. Critical Marangoni number versus volume ratio for liquid bridge ($\Gamma=1.0$, Pr=68.6).

III. NUMERICAL RESULTS

Figure 3 shows the dependency of the critical Marangoni number (listed in Table III) on the volume ratio for the liquid

TABLE III. Critical Marangoni number and azimuthal wave number versus volume ratio.

$\Gamma=1$			$\Gamma=1.6$		
V	10^4 Ma_c	m	V	10^4 Ma_c	m
0.60	1.86	1	0.60	0.686	1
0.65	7.02	1	0.65	0.707	1
0.67	12.3	1	0.70	0.789	1
0.68	13.9	1	0.75	1.00	1
0.69	15.6	1	0.78	1.34	1
0.70	18.4	1	0.80	1.77	1
0.71	18.0	1	0.81	4.62	0
0.72	18.2	1	0.82	4.82	0
0.73	26.4	1	0.83	5.21	0
0.74	24.0	1	0.84	6.04	0
0.75	21.7	1	0.85	7.37	1
0.77	18.0	1	0.90	5.21	1
0.80	14.4	1	1.00	3.29	1
0.85	10.6	1	1.10	2.92	1
0.90	7.97	1	1.20	3.10	1
1.00	5.09	1			
1.10	3.91	1			
1.20	3.47	1			

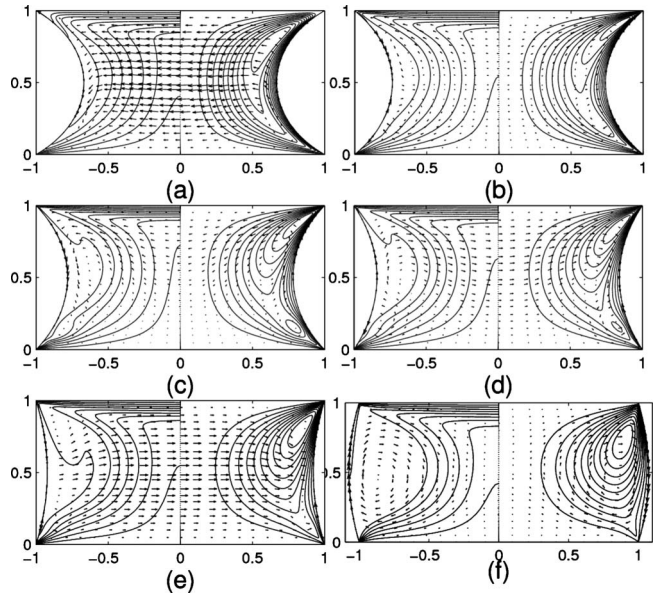

FIG. 4. Streamlines (solid lines at right half) and isotherms (solid lines at left half) of the basic state and velocity disturbance (vectors) at the corresponding critical Marangoni number for liquid bridge of ($\Gamma=1.0$, $\mathrm{Pr}=68.6$). (a) $V=0.6$, $\mathrm{Ma}_c=1.86\times10^4$, (b) $V=0.68$, $\mathrm{Ma}_c=1.39\times10^5$. (c) $V=0.73$, $\mathrm{Ma}_c=2.64\times10^5$, (d) $V=0.8$, $\mathrm{Ma}_c=1.44\times10^5$. (e) $V=0.9$, $\mathrm{Ma}_c=7.97\times10^4$, and (f) $V=1.1$, $\mathrm{Ma}_c=3.91\times10^4$.

bridge of $\Gamma=1.0$. With the increasing volume ratio, the marginal instability boundary consists of two branches, the steeply increasing branch in the range of volume ratios approximately less than 0.7 and the decreasing branch with a much flattened slope in the range of volume ratios approximately larger than 0.8. The strongly stabilized gap region can be clearly observed between the branches where the critical Marangoni number of the corresponding axisymmetric stationary thermocapillary convection drastically increases. Figure 4 shows the streamlines and isothermals of the basic state at the corresponding critical Marangoni number. For the cases of small volume ratio, $V=0.60$ for instance, the flow field consists of a single vortex with the vortex core close to the hot corner. When the volume ratio gets larger, $V=0.73$ for instance, the vortex core shifts towards the hot corner due to the development of a weak secondary vortex in the cold corner. When the volume ratio further increases till the transition to the case of convex free surface, $V=1.10$ for instance, the single-vortex flow pattern resumes while the vortex core shifts downwards and outwards to the center of the liquid bridge due to the increasing domain of the liquid column. The convective heat transfer plays a dominant role in liquid bridges of $\mathrm{Pr}=68.6$, and thermal boundary layer is developed in the neighbor region of the hot end while the isotherms in the cold corner is compressed. Note that in the parameter range studied, the critical azimuthal wave number of the oscillatory thermocapillary convection remains $m=1$. According to the study on cylindrical liquid bridges [10], the critical azimuthal wave number m of the oscillatory thermocapillary convection decreases with the increasing Pr number of the fluid, e.g., in a liquid bridge of unitary aspect ratio, the critical azimuthal wave number changes from $m=2$ to $m=1$ around $\mathrm{Pr}=28$. Similarly, for liquid bridges of $\mathrm{Pr}=68.6$ in the present study, the critical azimuthal wave number of $m\geq2$ does not occur.

For a deep insight into the energy transfer between the basic state and the disturbance of the thermocapillary convection, Fig. 5 shows the kinetic and "thermal" energy balances at the corresponding critical Marangoni numbers, which are normalized by the mechanical and thermal dissipation, respectively. In the kinetic-energy balance, the con-

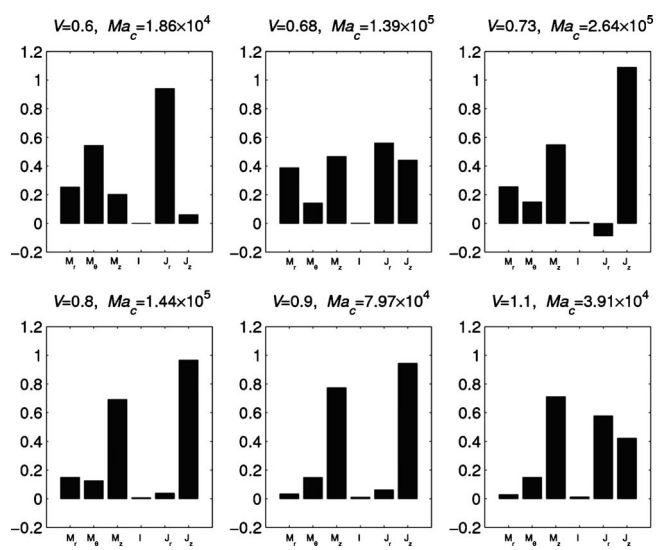

FIG. 5. Energy equilibrium of the disturbances for liquid bridge of ($\Gamma=1.0$, $\mathrm{Pr}=68.6$)

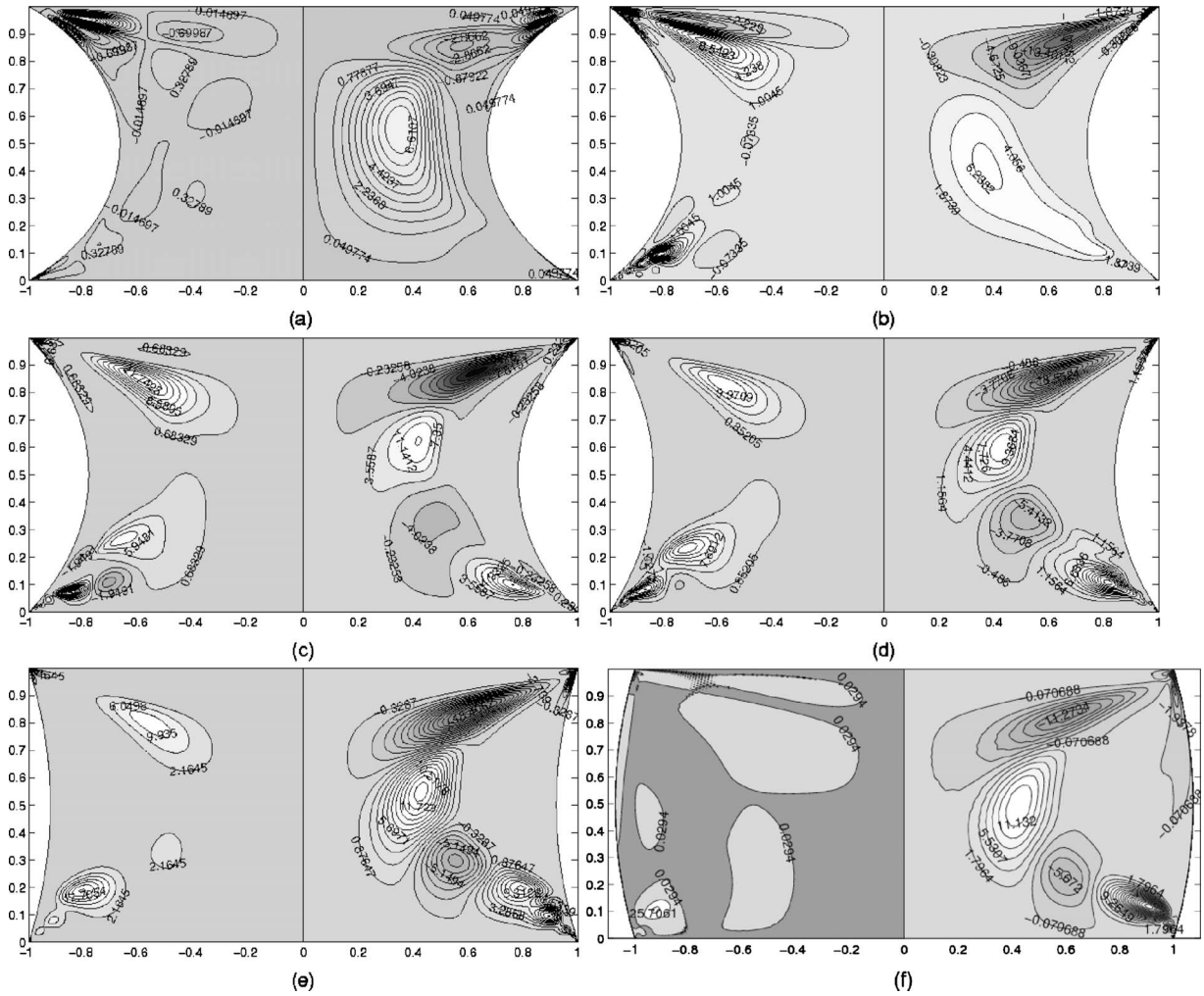

FIG. 6. Distribution density j_r of term J_r (right half), and j_z of term J_z (left half), in the "thermal energy" balance of disturbances for liquid bridge of ($\Gamma=1.0$, Pr=68.6). (a) $V=0.6$, $\mathrm{Ma}_c=1.86\times10^4$, (b) $V=0.68$, $\mathrm{Ma}_c=1.39\times10^5$, (c) $V=0.73$, $\mathrm{Ma}_c=2.64\times10^5$, (d) $V=0.8$, $\mathrm{Ma}_c=1.44\times10^5$, (e) $V=0.9$, $\mathrm{Ma}_c=7.97\times10^4$, and (f) $V=1.1$, $\mathrm{Ma}_c=3.91\times10^4$.

tribution from interaction between the stress tensor of the basic flow and the velocity disturbance (I) is negligible. The stabilizing effect is solely from the mechanical dissipation while the dominating destabilizing effect is from the work related to the thermocapillary force induced by the temperature disturbance on the free surface (M). Among its components, the contribution to the kinetic energy is mainly from (M_θ) associated with the work done by the azimuthal thermocapillary force in the cases of small volume ratios while (M_z) associated with the work done by the axial thermocapillary force becomes dominant in the cases of large volume ratios. On the other hand, the "thermal" energy balance is the emphasis of the investigation on liquid bridges of high-Pr fluids [3]. Figure 6 also shows the contours of j_r and j_z in the meridian plane of $\theta=\{0,\pi\}$. For the case of $V=0.60$, j_r is positive in most region of the liquid column and negative in the vicinity of the hot corner while j_z is weak in magnitude. Therefore, the destabilizing effect is mainly from the energy transfer to the temperature disturbance by the convective transport of the basic radial temperature distribution through the radial velocity disturbance (J_r) while the energy transfer by the convective transport of the axial temperature distribution through the axial velocity disturbance (J_z) is weak (see Fig. 5). With the increasing volume ratio, the negative component of j_r in the vicinity of the hot corner gets intensive, so do the positive components of j_z in the vicinity of the hot and cold corners. It results in the comparable contributions of J_r and J_z to the destabilizing effect. With the further increasing volume ratio into the gap region, an extra region of negative j_r occurs near the center of the liquid column and splits the region of positive j_r into two parts. Since the development of the negative components of j_r, especially the one in the vicinity of the hot corner, the general contribution of J_r to the destabilizing effect on the thermocapillary convection gets weak, even reverses to the stabilizing effect for the case of $V=0.73$. On the other hand, the positive components of j_z extends to the center of the liquid column and gets intensive, therefore, the general contribution of J_z to the destabilizing effect becomes dominant instead of J_r. When the volume ratio gets beyond unit, $V=1.10$ for instance, the significant shrinking of the major positive components of j_z to the hot and cold corners results in the comparable general contributions of J_r and J_z to the destabilizing effect again.

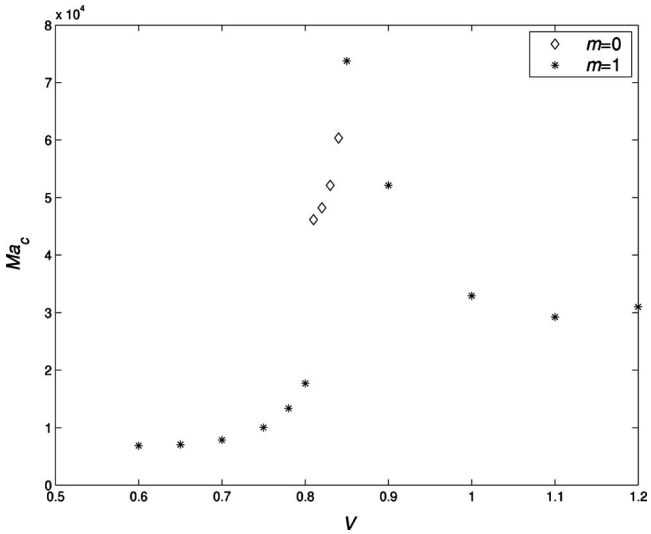

FIG. 7. Critical Marangoni number versus volume ratio for liquid bridge of ($\Gamma=1.6$, Pr=68.6).

Figure 7 shows the dependency of the critical Marangoni number (listed in Table III) on the volume ratio for the liquid bridge of $\Gamma=1.6$. It can be seen that with the increasing volume ratio, the marginal instability boundary also consists of the increasing branch and the decreasing branch, and a strongly stabilized gap region approximately exists in the range of volume ratios from 0.8 to 1.0. Compared to the case of $\Gamma=1.0$, the increasing branch is with a much flattened slope, and the gap region is broader and shifts to the larger volume ratio. Figure 8 shows the streamlines and isothermals of the basic state at the corresponding critical Marangoni number. Due to the relatively large aspect ratio, the flow field generally consists of two vortexes till the cases with large volume ratio implying the decreasing effect aspect ratio. It is worthy to be noted that a unique axisymmetric oscillatory thermocapillary convection with the critical azimuthal wave number of $m=0$ dominates the left sub-branch of the marginal instability boundary in the gap region while the critical azimuthal wave number for the rest cases is $m=1$. Figure 9 shows the corresponding distributions of the velocity disturbances on the horizontal cross section at $z=\frac{\Gamma}{2}$ with a time lag of half oscillation period indicating the axisymmetric oscillation mode without any azimuthal velocity disturbance.

Similar to the case of $\Gamma=1.0$, in the kinetic-energy balance (see Fig. 10), the major contribution to the destabilizing effect is from (M_θ) associated with the azimuthal thermocapillary force for the cases of small volume ratios and instead from (M_z) associated with the axial thermocapillary force becomes dominant with the increasing volume ratio. On the other hand, in the "thermal" energy balance, the contribution to the destabilizing effect by the energy transfer to the temperature disturbance by the convective transport of the basic radial temperature distribution through the radial velocity disturbance (J_r) overwhelms the energy transfer by the convective transport of the basic axial temperature distribution through the axial velocity disturbance (J_z). This situation remains until the volume ratio increases into the gap region where the contribution of J_z to the destabilizing effect grows rapidly and becomes dominant instead of J_r. When the volume ratio further increases beyond unit, the contributions of J_r and J_z to the destabilizing effect become comparable.

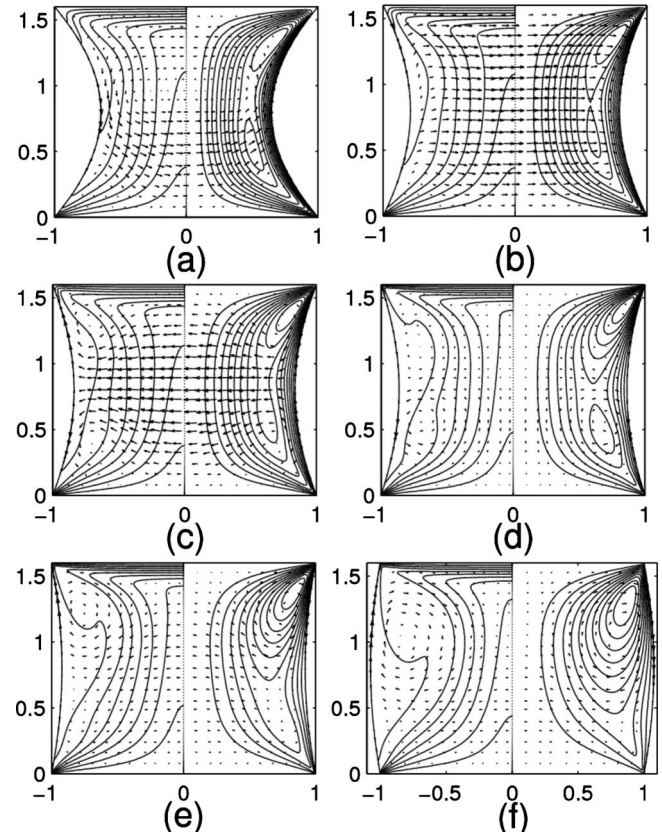

FIG. 8. Stream lines (solid lines at right half), isotherms (solid lines at left half) of the basic state and velocity disturbance (vectors) at the corresponding critical Marangoni number liquid bridge of ($\Gamma=1.6$, Pr=68.6). (a) $V=0.6$, $\mathrm{Ma}_c=6.86\times10^3$, (b) $V=0.75$, $\mathrm{Ma}_c=1.00\times10^4$, (c) $V=0.8$, $\mathrm{Ma}_c=1.77\times10^4$, (d) $V=0.83$, $\mathrm{Ma}_c=5.21\times10^4$, (e) $V=0.9$, $\mathrm{Ma}_c=5.21\times10^4$, and (f) $V=1.1$, $\mathrm{Ma}_c=2.92\times10^4$.

IV. CONCLUSIONS

In liquid bridges of 5cst silicon oil ($\Gamma=1.0$ and $\Gamma=1.6$), the transition of thermocapillary convection from the axisymmetric stationary flow to oscillatory flow is closely de-

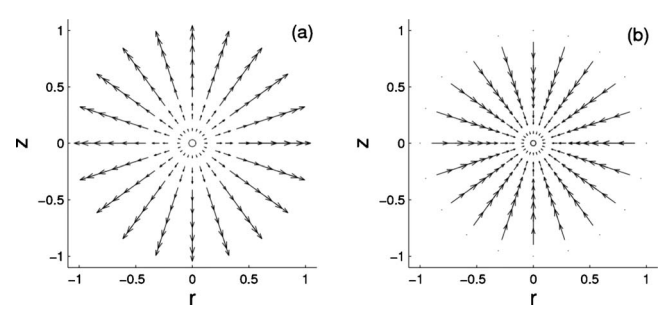

FIG. 9. Disturbance velocity on the horizontal plane at $z=\frac{\Gamma}{2}$ for liquid bridge of ($\Gamma=1.6$, Pr=68.6, and $V=0.83$) at $\mathrm{Ma}_c=5.21\times10^4$ (a) $t=T/2$ (b) $t=T$.

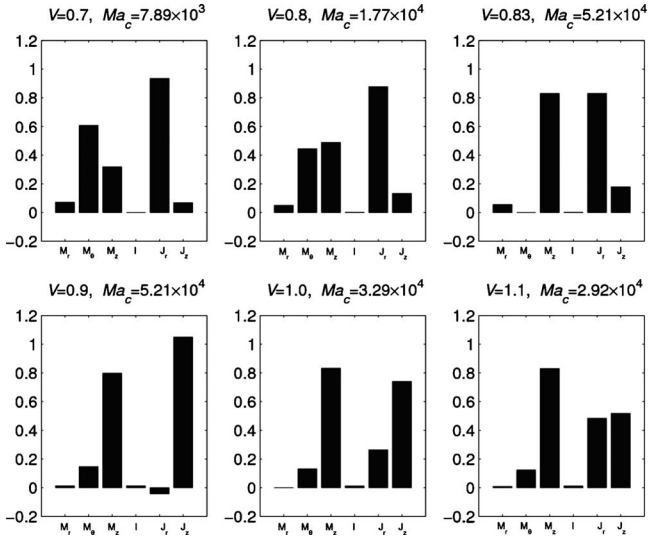

FIG. 10. Energy equilibrium of the disturbances for liquid bridge of ($\Gamma=1.6$, $\mathrm{Pr}=68.6$).

pendent on the volume ratio of liquid bridge. With the increasing volume ratio, the marginal instability boundary consists of the increasing branch and the decreasing branch with a gap region between them where the critical Marangoni number of the corresponding axisymmetric stationary flow increases drastically. Note that for the case of $\Gamma=1.6$, the gap region is relatively broader and shifts to the large volume ratio, and a unique oscillation mode of the thermocapillary convection with $m=0$ dominates the left subregime of the marginal instability boundary in the gap region.

The kinetic and "thermal" energy balances between the basic state and the disturbance of the thermocapillary convection are also volume-ratio dependent at the corresponding critical Marangoni number. The kinetic energy of the velocity disturbance is from the work done by the thermocapillary forces induced by the temperature disturbance on the free surface while the "thermal" energy of the temperature disturbance is from the basic thermal field through the convective transport by the velocity disturbance. In general, the energy of the disturbances is mainly from the basic thermal field: the velocity disturbance transports the energy from the basic thermal field to the temperature disturbance field, and the temperature disturbance on the free surface induces the thermocapillary forces which do work on the flow disturbance field. In this way, portion of the energy is transported from the temperature disturbance field to the velocity disturbance field, which enhances the above procedure, and finally the disturbances get intensive to provoke the instability. Moreover, the convective transport of the energy from the basic thermal field to the temperature disturbance by the velocity disturbance can be decomposed into two components, the one associated with the radial velocity disturbance (J_r) and the other one associated with the axial velocity disturbance (J_z). The destabilizing effect in the "thermal" energy balance is mainly from J_r in the range of small volume ratios while it is mainly from J_z in the stabilized gap region. The destabilizing effect is from both J_r and J_z in the range of large volume ratios. The hydrothermal wave instability suggested [12,13] in an infinite horizontal liquid film with return basic flow comes from the convective transport of the energy from the basic flow induced vertical temperature field to the temperature disturbance by the vertical velocity disturbance. If the same mechanism is applicable to the thermocapillary convection in the liquid bridge, the instability should be from J_r. In present study, the relative importance of J_r to J_z, however, is volume-ratio dependent. Therefore, due to the relative complexity of the basic thermocapillary convection in the liquid bridge, the corresponding instability mechanism is intricate and requires further investigations.

ACKNOWLEDGMENTS

This research was supported by Knowledge Innovation Project of the Chinese Academy of Sciences (Grant No. KJCX2-YW-L08) and the National Natural Science Foundation of China (Grant No. 10872202).

[1] Q. S. Chen and W. R. Hu, Int. J. Heat Mass Transfer **41**, 825 (1998).
[2] Q. S. Chen, W. R. Hu, and V. Prasad, J. Cryst. Growth **203**, 261 (1999).
[3] Ch. Nienhüser and H. C. Kuhlmann, J. Fluid Mech. **458**, 35 (2002).
[4] V. Shevtsova, J. Cryst. Growth **280**, 632 (2005).
[5] W. R. Hu, Z. M. Tang, and K. Li, Appl. Mech. Rev. **61**, 010803 (2008).
[6] H. C. Kuhlmann and H. J. Rath, J. Fluid Mech. **247**, 247 (1993).
[7] B. Xun, K. Li, P. G. Chen, and W. R. Hu, Int. J. Heat Mass Transfer **52**, 4211 (2009).
[8] G. Chen, A. Lizée, and B. Roux, J. Cryst. Growth **180**, 638 (1997).
[9] G. P. Neitzel, K. T. Chang, D. F. Jankowski, and H. D. Mittelmann, Phys. Fluids A **5**, 108 (1993).
[10] B. Xun, P. G. Chen, K. Li, Z. Yin, and W. R. Hu, Adv. Space Res. **41**, 2094 (2008).
[11] J.-K. Zhang, B. Xun, and P. G. Chen, Microgravity Sci. Technol. **21**, 111 (2009).
[12] M. K. Smith and S. H. Davis, J. Fluid Mech. **132**, 119 (1983).
[13] M. K. Smith, Phys. Fluids **29**, 3182 (1986).